doi:10.14311/ppt.2023.1.36
Plasma Physics and Technology **10**(1):36–39, 2023

STATISTICAL METHODS FOR IDENTIFYING SMALL DIFFERENCES IN THE THERMAL INTERRUPTION PERFORMANCE OF SF_6 ALTERNATIVES

J. Engelbrecht*, P. Pietrzak, D. Christen, P. Simka, C. Franck

High Voltage Laboratory, Swiss Federal Institute of Technology Zurich (ETHZ), 8092 Zurich, Switzerland

* jengelbre@ethz.ch

Abstract.

This contribution will present thermal current interruption measurements performed in pure CO_2 with a puffer circuit-breaker test device and establish a statistical method to assess the reignition probability as a function of the prospective current slope. Its efficacy will be demonstrated with measurements of the interruption limit scaling with respect to the pressure buildup inside the test device. A separate contribution will apply these methods to evaluate the influence of fluorinated additives on the switching performance [1].

Keywords: switching arcs, gas circuit breakers, thermal interruption, CO_2, SF_6 alternatives.

1. Introduction

A paradigm shift is underway in high-voltage power transmission, with long-standing SF_6-insulated designs being phased out in favor of alternatives with lower global warming potential. A number of proposed solutions for SF_6-free gas circuit-breakers use CO_2-based mixtures. In such mixtures the thermal switching behavior is mainly set by the CO_2 base gas, making the influence of additives challenging to detect experimentally. To investigate the switching processes in these mixtures, a test device based on the puffer circuit-breaker principle has been developed, enabling the study of pure gas properties under highly controlled conditions [2]. This contribution will present thermal interruption limit measurements performed with this device, and establish a statistical method to assess the reignition probability as a function of the prospective current slope. The method will be used to show that the interruption limit in CO_2 follows a blow pressure scaling of $3.1\frac{\mathrm{A}}{\mu\mathrm{s}\sqrt{\mathrm{bar}}}$. Using this approach, the interruption limit may be determined with an uncertainty much smaller than the scatter of individual test results, thereby allowing small changes in interrupting performance to be detected.

2. Methods

Experiments were performed using the setup shown in Fig. 1, introduced in [2]. A hydraulic drive acts to separate arcing contacts and compress a puffer volume. This generates a pressure difference Δp that blows cold gas through the arcing region inside a PMMA nozzle, cooling and extinguishing the arc at a current-zero (CZ) crossing. Measurements were performed in CO_2 at a fill pressure of 5 bar for four blow pressure (i.e. Δp) settings. Δp was varied by changing the opening speed of the drive via its throttle setting, while the timing of the drive trigger was adjusted such that the arc length measured by a linear potentiometer

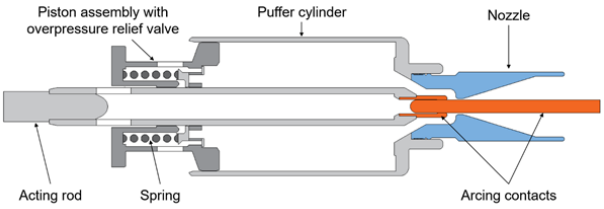

Figure 1. Interrupter region of puffer CB test device.

was always 43 ± 1 mm at the first CZ crossing. Using this method the pressure buildup may be controlled to within ±100 mbar, as measured by two transient pressure sensors located inside the puffer cylinder.

A synthetic test circuit was used to generate the test conditions: a high-current circuit (HCC) sustained the arc through the contact opening, and a current-injection circuit (CIC) controlled the $\mathrm{d}I/\mathrm{d}t$ at CZ and the transient recovery voltage (TRV) rise, at a fixed 450 Ω surge impedance. This setup allows conditions at CZ to be controlled with high reproducibility, independently of the peak HCC current, as the CIC settings determine the prospective $\mathrm{d}I/\mathrm{d}t$, while the puffer-breaker controls the pressure buildup with minimal influence from backheating. It should be noted that this setup produces a sustained TRV rise for at least 10 µs, a more prolonged voltage stress than would be applied in L90-like short-line fault (SLF) tests at the same $\mathrm{d}I/\mathrm{d}t$ and $\mathrm{d}u/\mathrm{d}t$, where the first line peak would occur within the first several µs [3].

To determine the thermal interruption limit, the applied $\mathrm{d}I/\mathrm{d}t$ and TRV must be varied while other conditions at the interruption instant are held constant. In practice, this was done according to the procedure introduced in [4]: the charging voltage of the CIC was varied in 1 kV increments between 15 kV to 30 kV, corresponding to changes in the prospective $\mathrm{d}I/\mathrm{d}t$ at CZ of approximately 0.33 A/µs over a range from 5 A/µs to 10 A/µs. Sets of 3–7 measurements

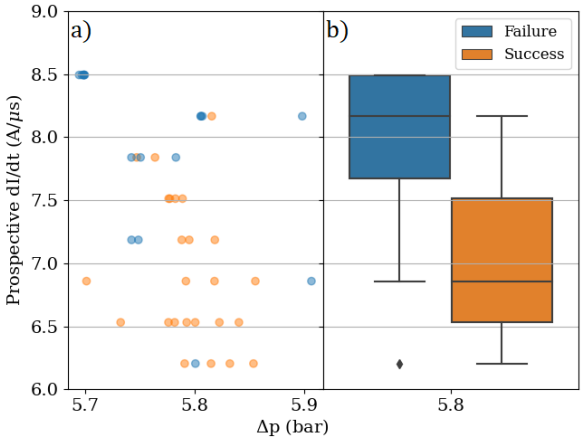

Figure 2. a) Scatter plot of 44 test outcomes in CO_2 as a function of blow pressure and prospective dI/dt (data points may overlap) b) Box-plot representation of measurement results.

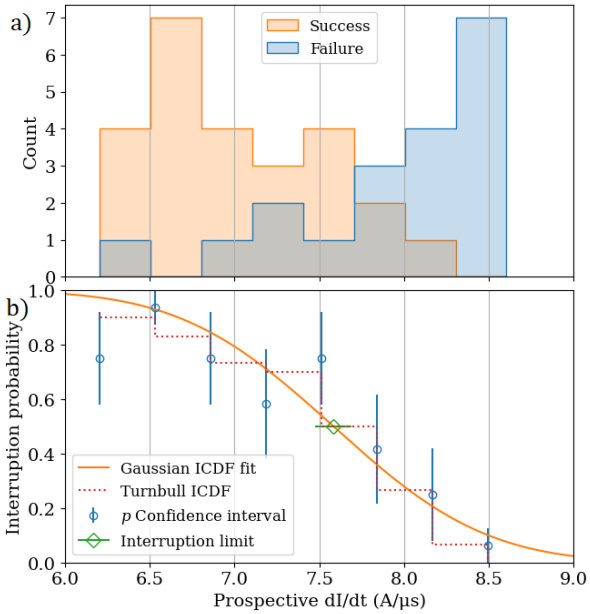

Figure 3. a) Histogram of thermal interruption test outcomes as a function of prospective dI/dt. b) Plot of estimated probability distribution and interruption limit determined from measurement results.

were performed at each setting, covering a range from 100% success rate to 100% failure rate, providing a good measure of the scatter of interruption outcomes.

3. Results & Discussion

3.1. Interruption Limit Determination

A scatter plot showing the outcome of each test performed for one pressure setting in CO_2 as a function of the prospective $\mathrm{d}I/\mathrm{d}t$ is presented in Fig. 2a, with interruption successes and failures indicated by color and plotted as a function of the measured blow pressure at CZ. Substantial scatter is evident, with both successes and failures occurring over a $2\,\mathrm{A/\mu s}$ range. In order to determine a limit value from this data, we define the limit as the $\mathrm{d}I/\mathrm{d}t$ at which there is an equal likelihood of a reignition or a successful interruption. The rate of change of the interruption probability with respect to $\mathrm{d}I/\mathrm{d}t$ should be maximized near this value, minimizing the uncertainty.

One method for determining the limit is with quantiles chosen to span the overlap of the two distributions. This can be visualized with the box-plot shown in Fig. 2b. Here the data from the scatter plot is grouped into two separate distributions for the interruption successes and failures. To examine only the influence of the prospective $\mathrm{d}I/\mathrm{d}t$, all tests are treated as having the same blow pressure of $5.8 \pm 0.1\,\mathrm{bar}$. The box-plot denotes the quartiles of both distributions: the colored regions represent the central 50%, bounded at the upper and lower quartiles, while the whiskers extend to the extrema of measured values that lie within 1.5 interquartile range of the central distribution, with outliers plotted individually. Taking the difference between the upper quartile of successes and the lower quartile of failures provides an estimated limit of $7.6\,\mathrm{A/\mu s}$ that can be perceived visually as the midpoint between the blue and orange boxes.

This approach provides a reliable measure of the interruption limit and a good representation of the scatter of test results, however it has several drawbacks. The method is somewhat sensitive to the sampling approach; e.g. if more measurements are performed under low $\mathrm{d}I/\mathrm{d}t$ conditions with a high likelihood of success than are performed at high $\mathrm{d}I/\mathrm{d}t$ where more failures are expected, the limit may be skewed to a lower $\mathrm{d}I/\mathrm{d}t$ value. This issue can be somewhat mitigated by a careful sampling approach centered on the interruption limit, but this requires foreknowledge of the expected limit and reduces flexibility during testing. The uncertainty of the limit is also difficult to quantify with this method, despite box-plots providing a good indication of the range in which the outcome of an individual test is uncertain.

To establish the uncertainty, it is useful to consider the data using statistical methods aimed at estimating the underlying probability distribution. Fig. 3a contains a histogram with the measurements from Fig. 2. Each bin contains one $\mathrm{d}I/\mathrm{d}t$ setting, and represents the outcome of n independent trials, each of which had nominally the same probability p of a successful interruption, resulting in n_S successes and n_F failures. The results in each bin are therefore described by the binomial distribution $B(n, n_\mathrm{S}, p)$, where p is a function of the prospective $\mathrm{d}I/\mathrm{d}t$.

With this description, an estimate for p and its uncertainty at each $\mathrm{d}I/\mathrm{d}t$ setting can be obtained using the so-called Wilson score interval [5],

$$p \approx \frac{n_\mathrm{S} + \frac{1}{2}z^2}{n + z^2} \pm \frac{z}{n + z^2}\sqrt{\frac{n_\mathrm{S} n_\mathrm{F}}{n} + \frac{z^2}{4}}, \qquad (1)$$

where z is set based on the target confidence level, taking a value of 1 for an interval spanning 1σ uncertainty. Several methods have been proposed for estimating

p, however the Wilson interval has ideal properties for describing the present experiment, namely that it may be reasonably applied to datasets with a low number of trials and/or values of p near 0 or 1 [6].

In Fig. 3b, estimated confidence intervals and values of p are plotted beneath the corresponding bins from the histogram, demonstrating lower uncertainty for settings with a higher number of trials. These points indicate the probability of interruption $p(\mathrm{d}I/\mathrm{d}t)$ with meaningful uncertainty, and form a distribution with empirically known properties. p should decrease monotonically with $\mathrm{d}I/\mathrm{d}t$, approaching 1 at low $\mathrm{d}I/\mathrm{d}t$ and 0 at high $\mathrm{d}I/\mathrm{d}t$. These properties describe an inverse cumulative distribution function (ICDF). To evaluate the interruption limit based on our estimated probabilities, we make the assumption that the underlying data is normally distributed and therefore can be fit with a Gaussian ICDF, with the points individually weighted by their uncertainties. This fit is shown in Fig. 3b, and corresponds to a normal distribution with a mean value $\mu = 7.6\,\mathrm{A/\mu s}$ and width $\sigma = 0.7\,\mathrm{A/\mu s}$. For comparison with this fit, an empirical ICDF that does not rely on assumptions about the distribution is also useful. Binary datasets do not translate directly to such an empirical representation, however one may be estimated using the method proposed by Turnbull, also plotted in Fig. 3b [7].

By definition, μ occurs at the $p = 0.5$ crossing of the ICDF and so corresponds to the thermal interruption limit. The uncertainty of the limit is then equivalent to $\sigma_\mu = \frac{\sigma}{n}$, the uncertainty in the mean of the distribution, and σ provides an indication of the scatter around this value, i.e. the region in which the outcome of an individual trial cannot be predicted to within 1σ confidence. Hence the method yields an interruption limit of $7.6 \pm 0.1\,\mathrm{A/\mu s}$ for CO_2 at a blow pressure of 5.8 bar, but indicates that for at least 84% certainty of a successful interruption, $\mathrm{d}I/\mathrm{d}t$ should not exceed $6.9\,\mathrm{A/\mu s}$.

3.2. Pressure Scaling in CO_2

To confirm the efficacy of this method, it was used to study the scaling of the thermal interruption limit in CO_2 with respect to the blow pressure at CZ. Pressure dependence has been studied thoroughly in SF_6 and shown to scale approximately with $\sqrt{p}$ [8], while theoretical models predict the same $\sqrt{p}$ scaling independent of blow gas [9]. Fig. 4 shows the results: the interruption limit determined using the binomial probability estimation method is plotted with error bars indicating the limit uncertainty σ_μ. Good agreement is observed between this method and the aforementioned box-plot quantile method, with all data points lying within the indicated uncertainty. Similar agreement is observed for the plotted fits to the function $a\sqrt{\Delta p}$, with both methods yielding values of $a = 3.1\,\frac{\mathrm{A}}{\mu\mathrm{s}\sqrt{\mathrm{bar}}}$. The expected scatter is indicated by the shaded blue region in this figure, determined by fitting the same $a\sqrt{\Delta p}$ function to $\mu + \sigma$ and $\mu - \sigma$, providing an uncertainty band that agrees with the experimentally observed scatter, as evidenced by the extrema indicated with orange error bars.

An interruption limit of $7.7\,\mathrm{A/\mu s}$ was determined for the highest investigated blow pressure of $\Delta p = 6.2$ bar. This finding is comparable to other values reported in literature: Uchii et al. showed a thermal interruption limit for CO_2 near $7.5\,\mathrm{A/\mu s}$ in the absence of significant nozzle ablation, however the blow pressure was not reported [10]. Stoller et al. determined a limit of approximately $11.2\,\mathrm{A/\mu s}$ at a higher blow pressure of $\Delta p = 11$ bar [11]; extrapolation of our fit predicts a slightly lower limit of $10.4\,\mathrm{A/\mu s}$ at this pressure. It should also be noted that this study assumed an interruption performance scaling with the square-root of the absolute stagnation pressure p_0, contrary to our findings, which suggest that the performance scales with $\sqrt{\Delta p}$. Fitting our data instead to $\sqrt{p_0}$ produces a noticeable mismatch, with the fit suggesting that the interruption performance should increase more slowly with blow pressure than is observed in our measurements. This disagreement lies well outside of our estimated uncertainty interval, however we note that several factors influencing the uncertainty have not been fully accounted for with the present approach, and will be discussed in the following section.

3.3. Discussion

Without further knowledge of the interruption probability distribution, the use of a normal distribution may be questioned. This assumption cannot be conclusively tested based on the limited number of experiments performed, however all results show good symmetry about $p = 0.5$, and the fits agree well with the estimated empirical ICDF. If the assumed distribution is incorrect, the calculated interruption limit may be affected, depending on the asymmetry of the real distribution about μ. Any influence resulting from such deviation should manifest as a systematic shift that similarly influences all results, such that relative comparisons between gases and other experimental parameters may still be made. Upcoming work will test this assumption by performing a large number of trials with the same experimental configuration, thereby allowing for both the long-term consistency of the results and the underlying probability distribution to be better characterized, affording higher confidence to the stated uncertainties.

Another influence which could not be completely controlled for throughout the pressure scaling comparison is the erosion of the PMMA nozzle. Tests were performed at reduced peak current, limiting erosion such that the pressure buildup at one experiment setting of ∼40 shots remained within the reported ±100 mbar uncertainty interval. It was thus inferred that erosion in the throat region of the nozzle was minimal, as previous measurements showed a decay in blow pressure at higher currents with more significant erosion. The same nozzle was then used to

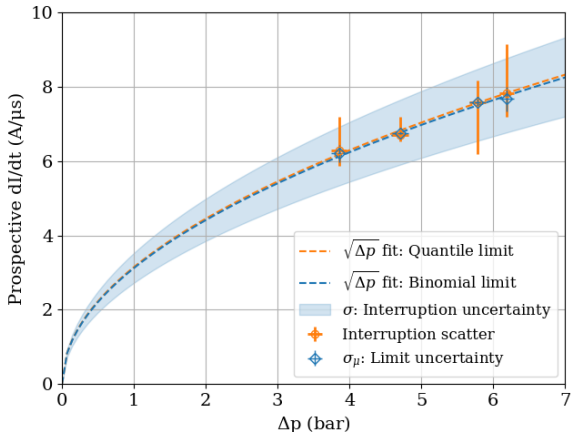

Figure 4. Pressure scaling of thermal interruption limit, and accompanying $\sqrt{\Delta p}$ fits.

perform tests at the different pressure settings. After the measurement series of ∼120 shots concluded, minor erosion of the throat and converging region of the nozzle was noted, suggesting that the average flow conditions experienced by the arc may have varied slightly between experimental settings. Looking ahead to measurements in other SF_6 alternative gas mixtures, comparisons will always be performed with a new, un-arced nozzle, and so should share comparable flow conditions over each measurement series.

In addition to these factors, our results show uncharacteristically late reignition times of up to 10 µs after CZ [4]. Analysis of voltage collapse waveforms, presented in [1], suggests the possibility of a different failure mechanism for the later reignitions, perhaps resulting from "hot dielectric" processes, as opposed to the classical understanding of thermal failures driven by runaway post-arc current heating. This finding raises the possibility that the present results underestimate the true thermal limit in CO_2, particularly for SLF switching duties where the first line peak occurs only a few µs after CZ. The alternative failure mechanism may also explain the observed differences in pressure scaling behavior.

4. Conclusions

A method has been demonstrated for determining the thermal interruption limit in a puffer circuit-breaker experiment by estimating the underlying probability distribution. The method was applied to interruption measurements in CO_2, and compared with a simpler approach based on the overlapping quantiles of interruption successes and failures. The two methods were shown to produce similar results, demonstrating that the interruption limit scales according to $3.1\frac{\mathrm{A}}{\mu\mathrm{s}\sqrt{\mathrm{bar}}}$ across the four blow pressures investigated. The probabilistic method allows for better estimation of the likelihood of a successful interruption at an arbitrary $\mathrm{d}I/\mathrm{d}t$ setting, and of the certainty with which the interruption limit may be determined based on the measurements. The suitability of this method is limited to experimental configurations where all test conditions are able to be reproduced to a high degree of precision, however it has been shown that in such conditions and with a sufficient number of trials, the interruption limit may be determined with a degree of certainty much higher than suggested by the width of the scatter. Such precision may prove invaluable when assessing the influence of minor changes to experimental parameters including gas mixture composition, arc length, and nozzle design.

Acknowledgements

The authors would like to thank Enrico Graneris, Fabian Mächler, Mahir Muratovic, and Martin Seeger for their valuable contributions to this work, which was made possible by financial support from Hitachi Energy Switzerland.

References

[1] P. Pietrzak et al. Thermal arc interruption performance of CO_2 and CO_2/C_4F_7N mixture. *To appear in 24th Symposium on Physics of Switching Arc*, 2023.

[2] C. Franck et al. Comparative Test Program Framework for Non-SF6 Switching Gases. *B&H Electrical Engineering*, 15:19–26, 2021. doi:10.3929/ethz-b-000508915.

[3] D. Peelo. *Current Interruption Transients Calculation*, chapter 5, pages 111–123. John Wiley & Sons, Ltd, 2020. ISBN 9781119547273. doi:10.1002/9781119547273.ch5.

[4] J. Engelbrecht et al. Evaluating conductance decay and post-arc current in axially blown CO_2 arcs. *To appear in Proc. of the XXIII Int. Conf. on Gas Discharges*, 2023.

[5] E. Wilson. Probable inference, the law of succession, and statistical inference. *Journal of the American Statistical Association*, 22(158):209–212, 1927. doi:10.1080/01621459.1927.10502953.

[6] S. Wallis. Binomial confidence intervals and contingency tests: Mathematical fundamentals and the evaluation of alternative methods. *Journal of Quantitative Linguistics*, 20(3):178–208, 2013. doi:10.1080/09296174.2013.799918.

[7] B. W. Turnbull. Nonparametric estimation of a survivorship function with doubly censored data. *Journal of the American Statistical Association*, 69(345):169–173, 1974.

[8] A. Plessl. The Influence of Pressure Profiles on Gas Blast Arc Interruption. *Proc. of the VII Int. Conf. on Gas Discharges*, pages 32–35, 1982.

[9] T. Christen and M. Seeger. Current interruption limit and resistance of the self-similar electric arc. *Journal of Applied Physics*, 97(10):106108, 2005. doi:10.1063/1.1913802.

[10] T. Uchii et al. Thermal interruption capability of CO_2 in a puffer-type circuit breaker utilizing polymer ablation. *IEEE/PES Transmission and Distribution Conference and Exhibition*, 3:1750–1754, 2002. doi:10.1109/TDC.2002.1177719.

[11] P. Stoller et al. CO2 as an Arc Interruption Medium in Gas Circuit Breakers. *IEEE Transactions on Plasma Science*, 41(8):2359–2369, Aug 2013. doi:10.1109/TPS.2013.2259183.